Numerical Solutions of Flow Past a Circular Cylinder at Reynolds Numbers up to 160

Jeongyoung Park*, Kiyoung Kwon and Haecheon Choi*,*****

(*Received March 14, 1998*)

Flow past a circular cylinder at Reynolds numbers up to 160 is simulated using high resolution calculations. Flow quantities at the cylinder surface are obtained and compared with those from the existing experimental and numerical studies. The present study reports the detailed information of flow quantities on the cylinder surface at low Reynolds numbers.

Key Words: Vortex Shedding, Circular Cylinder, Statistics on the Cylinder Surface

1. Introduction

Flow behind a circular cylinder has been a major research topic in fluid mechanics, not only because of the geometric simplicity but also because of the practical importance in engineering. At a very low Reynolds number ($Re=u_\infty d/\nu \ll 1$), flow around a circular cylinder is steady and symmetrical upstream and downstream, where u_∞ is the free-stream velocity, d the cylinder diameter and ν the kinematic viscosity. As the Reynolds number increases, the upstream-downstream symmetry disappears and two-attached eddies appear behind a cylinder. These eddies become bigger with increasing Reynolds number. For $Re>45$, unsteadiness arises spontaneously even though all the imposed conditions are being held steady and vortex shedding appears behind a circular cylinder (Tritton 1987). Accordingly, flow quantities on the cylinder surface significantly change as the Reynolds number increases. For example, when vortex shedding occurs behind a circular cylinder, drag on the cylinder increases and the body suffers from a periodic forcing in the normal direction to the main stream. This force sometimes makes the life of the structure shorten.

Since Roshko (1955) measured the vortex shedding period behind a bluff body, many investigators have measured and compared laminar vortex shedding frequencies (Strouhal number, $St=fd/u_\infty$) at low Reynolds numbers ($50<Re<200$), where f is the frequency. However, those results did not agree well with themselves. This was not because of the difficulty in measuring velocities in the wake but because of the difficulty in setting up the same experimental conditions. As pointed out in Williamson (1989), the existence of the discontinuity near $Re=70$ in the Strouhal and Reynolds number relation, which had been observed in several measurements, was due to the oblique vortex shedding. This discontinuity in the $St-Re$ relation disappeared when the vortex shedding was made to be parallel in the spanwise direction by introducing small plates at the end section of the cylinder. Therefore, it is not surprising to note that previous experimental and numerical results show some discrepancies among themselves.

There exist plenty of results from theoretical, experimental and numerical approaches for the flow behind a circular cylinder (see, for example, Oertel 1990; Williamson 1996), but few contain the detailed information of flow quantities on the cylinder surface. In the present study, we report a detailed information of all the flow quantities on the cylinder surface at low Reynolds numbers.

* Department of Mechanical Engineering, Seoul National University, Seoul 151-742, Korea
** Hyundai Motor Company, Whasung-Gun, Kyunggi-Do 445-850, Korea
*** Corresponding author: Tel: 82-2-880-8361; fax: 82-2-878-3662; e-mail: choi@socrates.snu.ac.kr

The flow quantities on the wall include the mean drag, drag and lift fluctuations, wall pressure and vorticity distributions, base pressure, separation angle, and length of eddies behind the cylinder. The Reynolds number investigated in this study ranges up to 160: according to the recent result by Mansy *et al.* (1994), three-dimensional flow behind a circular cylinder evolves from $Re \approx 150$. The results are compared with those of the existing experimental and numerical studies. The information of the flow quantities on the cylinder surface is of important value in understanding the flow physics as well as in checking the accuracy of an unsteady Navier-Stokes code in complex geometries. Note also that the flow variables on the cylinder surface is difficult to accurately measure at the low Reynolds numbers investigated in this study. Therefore, the present result will be also useful to checking the accuracy of an experimental measurement.

2. Computational Details

The governing equations for an incompressible flow can be written in the following form

$$\frac{\partial u_i}{\partial t}+\frac{\partial}{\partial x_j}u_iu_j=-\frac{\partial p}{\partial x_i}+\frac{1}{Re}\frac{\partial}{\partial x_j}\frac{\partial}{\partial x_j}u_i, \quad (1)$$

$$\frac{\partial u_i}{\partial x_i}=0, \quad (2)$$

where x_i are the Cartesian coordinates, and u_i are the corresponding velocity components. All variables are non-dimensionalized by the cylinder diameter d and the free-stream velocity u_∞. Re denotes the Reynolds number, defined as $Re=u_\infty d/\nu$.

Eqs. (1) and (2) are rewritten in a conservative form in generalized coordinates. The dependent variables in the transformed Navier-Stokes equations are volume fluxes across the faces of the cells, which are equivalent to using the contravariant velocity components on a staggered grid multiplied by the Jacobian of the coordinate transformation, J. Using this choice, the discretized mass conservation can be easily satisfied (Rosenfeld *et al.* 1991; Choi *et al.* 1992, 1993). The terms in the transformed equations are described in detail in Choi *et al.* (1992).

The integration method used to solve the transformed equations is based on a fully implicit, fractional step method (Choi and Moin 1994; Hahn and Choi 1997). All terms including cross-derivative diffusion terms are advanced with the Crank-Nicolson method in time, and are resolved with the second-order central-difference scheme in space. A Newton-iterative method is used to solve the discretized nonlinear equations.

The flow geometry and coordinate system along with boundary conditions are shown in Fig. 1. In this study we use a C-grid system that is known for better resolution in the wake region than an O-grid system (Thompson *et al.* 1985). The periodic boundary condition is used at the branch cut and a convective outflow condition is used for the outflow boundary condition (Pauley *et al.* 1990). This boundary condition allows vortices to smoothly pass away from the computational domain. A Dirichlet boundary condition, $u=u_\infty$ and $v=0$, is used at far-field boundaries, and the no-slip condition is applied on the cylinder surface.

The computational domain used is $-50d<x<20d$ and $-50d<y<50d$, where $(x=0, y=0)$ corresponds to the center location of the cylinder. A non-uniform mesh of 641×241 points is created using a hyperbolic grid generation technique.

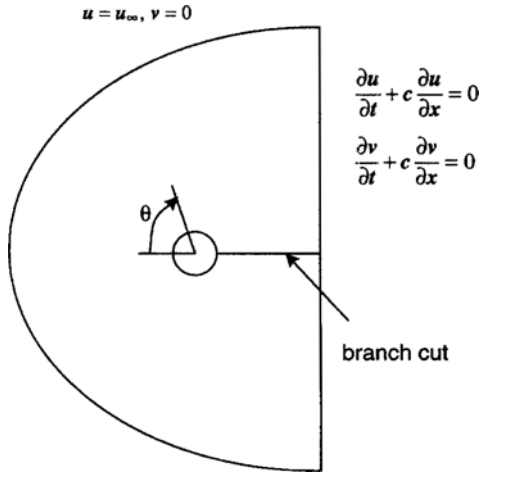

Fig. 1 Flow geometry and coordinate system along with boundary conditions. Here c is the average exit velocity.

128 grid points are located on the cylinder surface. The current mesh and domain size have been determined from an extensive study of the numerical parameters (e. g., computational domain size, number of grid points, skewness of the computational mesh, etc.). We have found from this study that the domain size in the cross-streamwise (y) direction is more critical in accurately predicting the Strouhal number than the domain size in the streamwise (x) direction. Doubling the domain size in both directions changed the predicted Strouhal number by less than 0.5 % and reducing the number of grid points by half does not change the Strouhal number.

For all cases investigated in this paper, we have used the computational time step, $\Delta t u_\infty/d=0.03$, which corresponds to $CFL\approx 4$. About 3 Newton iterations were needed to solve the discretized nonlinear momentum equations. We have also simulated the flow with the half time step ($\Delta t u_\infty/d=0.015$), which resulted in only 0.2% change of the predicted Strouhal number. The CPU time required was about 5 CRAY YMP C90 seconds per time step. Figure 2 shows the Strouhal number as a function of the Reynolds number. The Strouhal number obtained in this study is compared with those of Williamson (1989), Norberg (1994) and other numerical results. An excellent agreement is found between the present study and the experimental results. In the present study, vortex shedding starts from $Re=47$.

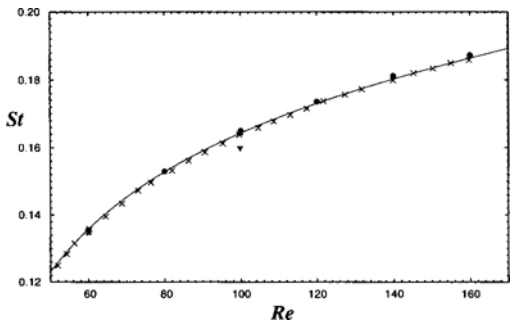

Fig. 2 Strouhal number vs. Reynolds number: ●, present study; ———, $St=-3.3265/Re+0.1816+1.6\times10^{-4}Re$ (Williamson 1989); ×, Norberg (1994); ▼, Braza *et al.* (1986); ▲, Park *et al.* (1994).

3. Results

In this section, we report the detailed information of flow quantities on the cylinder surface at low Reynolds numbers. In cases of unsteady flow ($Re\geq 47$), flow quantities are averaged in time.

Figure 3 shows the distribution of the time-averaged wall pressure coefficient, $C_p=(p-p_\infty)/\left(\frac{1}{2}\rho u_\infty^2\right)$, where p_∞ is the free-stream pressure. They are in good agreement with those of Dennis and Chang (1970) at $Re<45$ and in a rough agreement with the experimental result of Norberg (1993).

Figure 4 shows the pressure coefficients at the stagnation and base points as a function of the Reynolds number. It is interesting to note that the

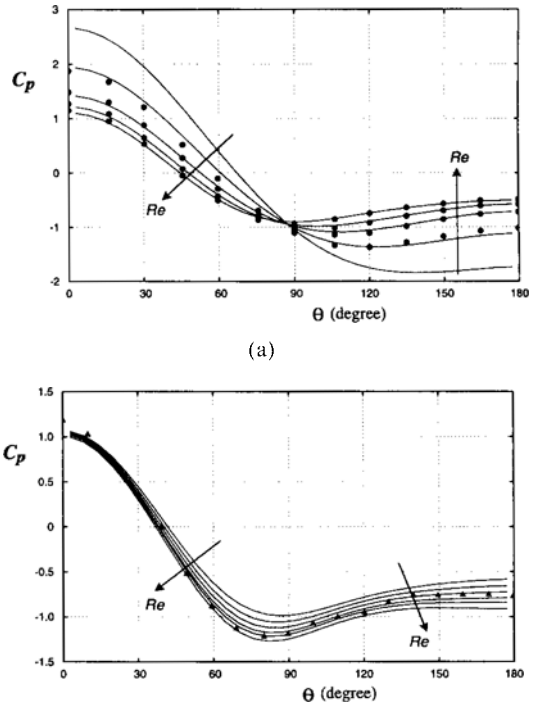

Fig. 3 Time-averaged wall pressure coefficient: (a) $Re=2$, 4, 10, 20, 40; (b) $Re=60$, 80, 100, 120, 140, 160, ●, $Re=5$, 10, 20, 40 (Dennis and Chang 1970); ▲, $Re=130$ (Norberg 1993). $\theta=0°$ and $\theta=180°$ correspond to the stagnation and base points of the cylinder, respectively.

Table 1 Drag and lift coefficients.

Re	C_D	C_{Dp}	$\hat{C}_D$	$\hat{C}_{Dp}$	$\hat{C}_{Df}$	$\hat{C}_L$	$\hat{C}_{Lp}$	$\hat{C}_{Lf}$
2	6.85	3.48	-	-	-	-	-	-
4	4.53	2.37	-	-	-	-	-	-
10	2.78	1.56	-	-	-	-	-	-
20	2.01	1.21	-	-	-	-	-	-
40	1.51	0.99	-	-	-	-	-	-
60	1.39	0.96	0.0014	0.0012	0.0002	0.1344	0.1149	0.0226
80	1.35	0.97	0.0049	0.0043	0.0006	0.2452	0.2145	0.0343
100	1.33	0.99	0.0091	0.0082	0.0010	0.3321	0.2949	0.0417
120	1.32	1.01	0.0152	0.0139	0.0015	0.4103	0.3684	0.0470
140	1.32	1.03	0.0224	0.0206	0.0020	0.4823	0.4368	0.0511
160	1.32	1.04	0.0293	0.0270	0.0025	0.5501	0.5020	0.0543

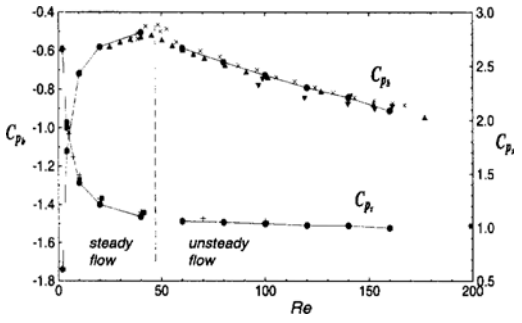

Fig. 4 Stagnation pressure coefficient C_{p_s} and base pressure coefficient C_{p_b}: ●, present study; +, Dennis and Chang (1970); ■, Fornberg (1980); ×, Williamson and Roshko (1990); ▼, Norberg (1994); ▲, Henderson (1995).

stagnation pressure monotonically decreases as the Reynolds number increases, while the base pressure shows a non-monotonic behavior. That is, as Re increases, the base pressure increases in steady flow, but it decreases when flow becomes unsteady. Because the base pressure is very sensitive to the dynamics of wake, it has often been used in the presentation of instabilities for the flow past a circular cylinder. Excellent agreement is found among the data shown in Fig. 4.

Table 1 shows the drag and lift coefficients at the Reynolds numbers investigated, where $\hat{(\ )}$ denotes the amplitude of a flow quantity, maximum deviation from the time averaged value during a period. C_D and C_{Dp} are the total drag and pressure drag coefficients and C_L is the lift coefficient. The friction drag coefficient is $C_{Df} = C_D - C_{Dp}$. It is shown that the contribution of the pressure drag to the total drag becomes larger

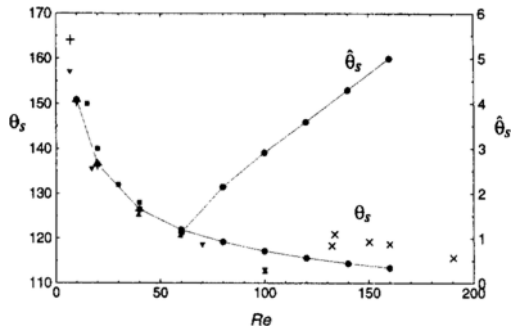

Fig. 5 Mean separation angle and amplitude of the separation angle fluctuations: ●, present study; ×, Grove *et al.* (1964); +, Dennis and Chang (1970); ■, Coutanceau and Bouard (1977); ▼, Tuann and Olson (1978); ▲, Braza *et al.* (1986). $\theta = 0°$ and $\theta = 180°$ correspond to the stagnation and base points of the cylinder, respectively.

than that of the friction drag as Re increases. Also, as Re increases, the total drag coefficient monotonically decreases, while the pressure drag coefficient decreases in steady flow but increases in unsteady flow, indicating that vortex shedding significantly increases the pressure drag. It is clear from Table 1 that the drag and lift fluctuations occur mainly from the pressure fluctuations and increase as Re increases. Also, the lift fluctuations are much bigger than the drag fluctuations. Note that $\hat{C}_L \neq \hat{C}_{Lp} + \hat{C}_{Lf}$ (see Table 1) because the maximum deviations of the lift components due to the pressure and friction fluctuations occur at different times.

Figure 5 shows the mean separation angle and the amplitude of the separation angle fluctuations as a function of the Reynolds number. At $Re < 100$, there is a good agreement among the data, while at $Re \geq 100$, the present result locates in between the existing ones. As Re increases, the fluctuations of the separation angle increase due to stronger vortex shedding.

Figure 6 shows the time-averaged separation bubble length, which is the distance from the base of the cylinder to the point where the time-averaged streamwise velocity is zero. Before the onset of vortex shedding, a good agreement is observed among the data. However, after the onset of vortex shedding, a difference is observed. In

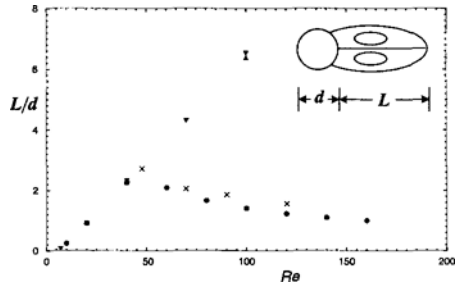

Fig. 6 Length of the time-averaged separation bubble behind cylinder vs. Reynolds number: ●, present study; ▼, Dennis and Chang (1970); ×, Nishioka and Sato (1978); ▲, Fornberg (1980).

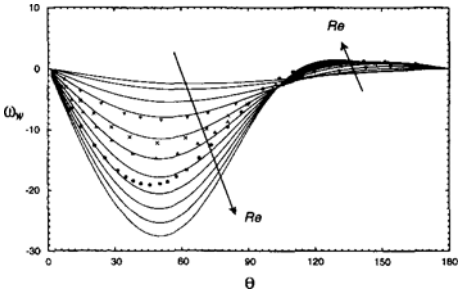

Fig. 7 Wall vorticity: ———, Re = 2, 4, 10, 20, 40, 60, 80, 100, 120, 140, 160 (present study); ▼, Re=20, ×, Re=40, ▲, Re=60, ●, Re =100 (Braza *et al.* 1986).

steady solutions of the Navier-Stokes equations, a linear increase of the bubble length with Re is observed (Dennis and Chang 1970; Fornberg 1980). In experiments of Nishioka and Sato (1974, 1978), when the aspect ratio (cylinder length/diameter) was small (6.5), vortex shedding was suppressed and a linear increase of the bubble length was observed. However, when the aspect ratio was 67, they obtained results shown in Fig. 6. The present result shows a fair agreement with Nishioka and Sato (1978).

The distribution of the wall vorticity is shown in Fig. 7, together with numerical results of Braza *et al.* (1986). Disagreement of the present data with Braza *et al.* becomes bigger as Re increases. This seems to be due to the insufficient resolution used in Braza *et al.* at higher Reynolds numbers (see also Figs. 2 and 5): the number of grid points used in Braza *et al.* was about 13,000, while that of the present study is about 150,000.

4. Summary

Flow past a circular cylinder at Reynolds numbers up to 160 was simulated using high resolution unsteady calculations. Flow quantities including the Strouhal number, coefficients of the drag, lift and base pressure, wall pressure and vorticity distributions, separation angle, and length of the separation bubble were reported as a function of the Reynolds number. Most of the results showed good agreement with previous experimental and numerical results. The information of flow quantities on the cylinder surface should be valuable in understanding the flow physics as well as in checking the accuracy of an unsteady Navier-Stokes code in complex geometries.

Acknowledgement

This research was supported by SNU Engineering Education and Research Foundation and by Creative Research Initiatives of the Korean Ministry of Science and Technology. We gratefully acknowledge the supports.

References

Braza, M., Chassaing, P. and Ha Minh, H., 1986, "Numerical Study and Physical Analysis of the Pressure and Velocity Fields in the Near Wake of a Circular Cylinder," *J. Fluid Mech.*, Vol. 165, pp. 79~130.

Choi, H., Moin, P. and Kim, J., 1992, "Turbulent Drag Reduction: Studies of Feedback Control & Flow over Riblets," Report No. TF-55. Department of Mechanical Engineering, Stanford University, Stanford, CA.

Choi, H., Moin, P. and Kim, J., 1993, "Direct Numerical Simulation of Turbulent Flow over Riblets," *J. Fluid Mech.*, Vol. 255, pp 503~539.

Choi, H. and Moin, P., 1994, "Effects of the Computational Time Step on Numerical Solutions of Turbulent Flow," *J. Comp. Phys.*, Vol. 113, pp. 1~4.

Coutanceau, M. and Bouard, R., 1977, "Experi-

mental Determination of the Main Features of the Viscous Flow in the Wake of a Circular Cylinder in Uniform Translation. Part 1. Steady Flow," *J. Fluid Mech.*, Vol. 79, pp. 231~256.

Dennis, S. C. R. and Chang, G., 1970, "Numerical Solutions for Steady Flow Past a Circular Cylinder at Reynolds Numbers up to 100," *J. Fluid Mech.*, Vol. 42, pp. 471~489.

Fornberg, B., 1980, "A Numerical Study of Steady Viscous Flow past a Circular Cylinder," *J. Fluid Mech.*, Vol. 98, pp. 819~855.

Grove, A. S., Shair, F. H., Petersen, E. E., and Acrivos, A., 1964, "An Experimental Investigation of the Steady Separated Flow past a Circular Cylinder," *J. Fluid Mech.*, Vol. 19, pp. 60~80.

Hahn, S. and Choi, H., 1997, "Unsteady Simulation of Jets in a Cross Flow," *J. Comp. Phys.*, Vol. 134, pp. 342~356.

Henderson, R. D., 1995, "Details of the Drag Curve near the Onset of Vortex Shedding using High-resolution Computer Simulation," *Phys. Fluids*, Vol. 7, pp. 2102~2104.

Mansy, H., Yang, P. and Williams, D. R., 1994, "Quantitative Measurements of Three-dimensional Structures in the Wake of a Circular Cylinder" *J. Fluid Mech.*, Vol. 270, pp. 277~296.

Nishioka, M. and Sato, H., 1974, "Measurements of Velocity Distributions in the Wake of a Circular Cylinder at Low Reynolds Numbers," *J. Fluid Mech.*, Vol. 65, pp. 97~112.

Nishioka, M. and Sato, H., 1978, "Mechanism of Determination of the Shedding Frequency of Vortices behind a Cylinder at Low Reynolds Numbers," *J. Fluid Mech.*, Vol. 89, pp. 49~60.

Norberg, C., 1993, "Pressure Forces on a Circular Cylinder in Cross Flow," In *Proc. IUTAM Symp. Bluff-Body Wakes, Dynamics and Instabilities, 7-11 September 1992, Göttingen*, 275. Springer.

Norberg, C., 1994, "An Experimental Investigation of the Flow around a Circular Cylinder: Influence of Aspect Ratio," *J. Fluid Mech.*, Vol. 258, pp. 287~316.

Oertel, H., 1990, "Wakes behind Blunt Bodies," *Annu. Rev. Fluid Mech.*, Vol. 22, pp. 539~564.

Park, D. S., Ladd, D. M. and Hendricks, E. W., 1994, "Feedback Control of von Karman Vortex Shedding behind a Circular Cylinder at Low Reynolds Number," *Phys. Fluids*, Vol. 6, pp. 2390~2405.

Pauley, L. L., Moin, P. and Reynolds, W. C., 1990, "The Structure of Two-dimensional Separation," *J. Fluid Mech.*, Vol. 220, pp. 397~411.

Rosenfeld, M., Kwak, D. and Vinokur, M., 1991, "A Fractional Step Solution Method for the Unsteady Incompressible Navier-Stokes Equations in Generalized Coordinate Systems," *J. Comp. Phys.*, Vol. 94, pp. 102~137.

Roshko, A., 1955, "On the Wake and Drag of Bluff Bodies," *J. Aeronaut. Sci.*, Vol. 22, pp. 124~132.

Thompson, J. F., Warsi, Z. U. A. and Mastin, C. W., 1985, *Numerical Grid Generation-Foundations and Application*, Elsevier Science Publishing Co., New York.

Tritton, D. J., 1987, *Physical Fluid Dynamics*, Oxford University Press, Oxford.

Tuann, S.-Y. and Olson, M. D., 1978, "Numerical Studies of the Flow around a Circular Cylinder by a Finite Element Method," *Comp. Fluids*, Vol. 6, p. 219.

Williamson, C. H. K., 1989, "Oblique and Parallel Modes of Vortex Shedding in the Wake of a Circular Cylinder at Low Reynolds Numbers," *J. Fluid Mech.*, Vol. 206, pp. 579~627.

Williamson, C. H. K., 1996, "Vortex Dynamics in the Cylinder Wake," *Annu. Rev. Fluid Mech.*, Vol. 28, pp. 477~539.

Williamson, C. H. K. and Roshko, A., 1990, "Measurements of Base Pressure in the Wake of a Cylinder at Low Reynolds Numbers," *Z. Flugwiss. Weltraumforsch.* Vol. 14, pp. 38~46.